Relationship between the magnetic moment of Lu and the magnetic behavior of $(Y_yLu_{1-y})(Co_{1-x}Al_x)_2$ from x-ray absorption spectroscopy and x-ray magnetic circular dichroism

J. Chaboy,[1] M. A. Laguna-Marco,[2] C. Piquer,[1] H. Maruyama,[3] N. Kawamura,[4] N. Ishimatsu,[3]
M. Suzuki,[4] and M. Takagaki[4]

[1]*Instituto de Ciencia de Materiales de Aragón, CSIC—Universidad de Zaragoza, 50009 Zaragoza, Spain*
[2]*CITIMAC, Universidad de Cantabria, Avenida de los Castros s/n, 39005 Santander, Spain*
[3]*Graduate School of Science, Hiroshima University, 1-3-1 Kagamiyama, Higashi-Hiroshima 739-8526, Japan*
[4]*Japan Synchrotron Radiation Research Institute, 1-1-1 Kouto, Mikazuki, Sayo, Hyogo 679-5148, Japan*

We present an x-ray magnetic circular dichroism (XMCD) study performed at both the Co K edge and the Lu $L_{2,3}$ edges on $(Y_yLu_{1-y})(Co_{1-x}Al_x)_2$ systems. The XMCD spectra reflect the different magnetic character of these systems, allowing us to monitor the transition from weak to strong ferromagnetism. The XMCD at the Lu $L_{2,3}$ edges indicates the existence of an ordered $5d$ moment at the lutetium sites that is coupled antiparallel to the Co moment. Estimates of the magnetic moment of Lu have been obtained by applying the XMCD sum rules. Our results show that there is a correlation between the Lu $5d$–induced magnetic moment and the magnetic character of the $(Y_yLu_{1-y})(Co_{1-x}Al_x)_2$ compounds. These results suggest that the developing of the Lu moment plays an important role in reinforcing the magnetic interactions and favoring the ferromagnetic character of the Lu-rich compounds.

PACS number(s): 75.50.Cc, 75.30.Kz, 61.10.Ht, 87.64.Ni

I. INTRODUCTION

The intermetallic RCo_2 compounds (R stands for rare-earth elements) are particularly interesting to study the magnetism of $3d$ and $4f$ metals as the Co moment strongly depends upon the R alloying component.[1,2] These intermetallic compounds are characterized by the occurrence of a metamagnetic transition in the Co $3d$ itinerant subsystem and by the dependence of the Co magnetic moment on the R alloying component. For compounds in which R is nonmagnetic (YCo_2, $LuCo_2$) the Co susceptibility is of the Pauli type, while in the case of compounds with magnetic R metals, a Co moment $\sim 1\mu_B$ is induced. The magnetic order of the d subsystem in the RCo_2 compounds with magnetic R is due to the effect of the molecular field acting on the Co sites (H_{fd}).

Another peculiarity of this family comes from the fact that substitution of Co by a nonmagnetic atom as Al induces ferromagnetic order. YCo_2 is a typical exchange-enhanced Pauli paramagnet and the occurrence of a ferromagnetic state takes place upon applying a critical field $B_c = 69$ T at $T = 10$ K.[1,3] The critical field of the metamagnetic transition, B_c, decreases in the $Y(Co_{1-x}Al_x)_2$ series as Co is replaced by nonmagnetic Al. Weak ferromagnetism occurs for $0.12 < x < 0.20$ compounds, the spontaneous Co magnetic moment being $\mu_{Co} \sim 0.1\mu_B$. Within this series both the maximum spontaneous moment $\sim 0.14\mu_B/$Co and the maximum Curie temperature $T_C \sim 25$ K correspond to the $x \simeq 0.15$ compound.[4,5] Moreover, these systems exhibit transitions from weak (WFM; $\mu_{Co} \sim 0.1\mu_B$) to strong ferromagnetism (SFM; $\mu_{Co} \sim 0.6\mu_B$) under high magnetic fields.[6–9]

This behavior has been attributed to the modification of the $3d$ density of states (DOS) whose shape near the Fermi level E_F is rather peculiar.[10,11] In this way, different hypotheses have been formulated to account for the impact of Al on the magnetic properties of YCo_2. On the one hand, several authors argue that the increase of the lattice parameter due to

Al leads to both a narrowing of the bandwidth and an increase of the density of states at the Fermi level, $N(E_F)$.[4] By contrast, it has also been postulated that the increase of $N(E_F)$ comes from a decrease in the density of $3d$ electrons produced by the substitution of Co ($3d^7$ configuration) by $Al(3d^0)$.[12] However, neither of the above interpretations takes into account the change of the DOS near E_F due to Al substitution. Theoretical band calculations suggest that the strong hybridization between the Co($3d$) and Al($3p$) bands modifies the shape of the characteristic peak of the YCo_2 DOS in such a way that upon increasing Al content $N(E_F)$ increases and weak ferromagnetism is favored.[13,14] Additional support to this hypothesis is given by x-ray photoelectron spectroscopy measurements,[15] suggesting the lowering of E_F with Al substitution, and by the modification of the magnetic behavior of YCo_2 upon doping with Fe and Ni.[16] More recently, band calculations reported by Khmelevskyi *et al.* have shown that the increase of the DOS at the Fermi energy in the $Y(Co_{1-x}Al_x)_2$ system is a direct consequence of the smoothing of the DOS peaks due to the substitution of Co by Al.[17]

Research was extended to the case of $Lu(Co_{1-x}Al_x)_2$ in which Lu, like yttrium, bears no $4f$ magnetic moment,[12,18,19] and $(Y_{1-y}Lu_y)(Co_{0.88}Al_{0.12})_2$, in which the crystal cell parameter is kept constant and similar to that of YCo_2.[12,18] These studies reveal that the influence of Al on the magnetic properties of Y and Lu compounds is rather different. Indeed, the $Lu(Co_{1-x}Al_x)_2$ compounds show SFM behavior for the same concentration at which the $Y(Co_{1-x}Al_x)_2$ compounds become WFMs.[12,18,20] Moreover, by contrast to the Y case, the $Lu(Co_{1-x}Al_x)_2$ systems exhibit a sharp metamagnetic transition without showing a remarkable change in magnitude of the field-induced moment.[19,21] In the case of the $(Y_{1-y}Lu_y)(Co_{0.88}Al_{0.12})_2$ compounds it was found that the magnetic ground state changes from WFM (in Y-rich compounds) to SFM (in Lu-rich compounds) within a narrow

concentration range in the vicinity of $y=0.4$.[22] Moreover, no metamagnetic transitions are observed for the Lu-rich compounds.[19] This behavior cannot be explained in terms of a rigid band model and it has been qualitatively interpreted in terms of the different hybridization between Co($3d$) and Y($4d$) and Co($3d$) and Lu($5d$).[19,21,23]

Aiming to furnish direct information about the modification of the electronic structure induced by Al in both Y and Lu compounds, we have performed a combined x-ray absorption spectroscopy (XAS) and x-ray magnetic circular dichroism (XMCD) study of the Y(Co$_{1-x}$Al$_x$)$_2$, Lu(Co$_{1-x}$Al$_x$)$_2$, and (Y$_y$Lu$_{1-y}$)(Co$_{0.88}$Al$_{0.12}$)$_2$ series. In this way, both the Co K edge and the Lu $L_{2,3}$ edge XAS and XMCD have been measured through the paramagnetic-WFM-SFM transitions in the (Y$_y$Lu$_{1-y}$)(Co$_{1-x}$Al$_x$)$_2$ series. In addition, XMCD sum rules[24,25] have been applied to the Lu $L_{2,3}$ edge spectra to determine the existence of a magnetic moment at the Lu sites and its relationship with the different, WFM vs SFM, magnetic behavior of the Y- and Lu-based compounds.

II. EXPERIMENT

Y(Co$_{1-x}$Al$_x$)$_2$ ($x=0.06$, 0.10, 0.11, 0.13, 0.15, and 0.20), Lu(Co$_{0.9}$Al$_{0.1}$)$_2$, and (Y$_{1-y}$Lu$_y$)(Co$_{0.88}$Al$_{0.12}$)$_2$ ($y=0.2$, 0.4, and 0.6) samples were prepared by arc-melting the pure elements under Ar protective atmosphere following standard procedures.[4,12,18] The ingots were annealed at 850 °C for one week. Structural characterization was performed at room temperature by means of powder x-ray diffraction by using a rotating-anode Rigaku diffractometer in the Bragg-Brentano geometry, with Cu $K\alpha$ radiation. The diffraction patterns, analyzed by using the FULLPROF code,[26] showed that all the samples are single phase, corresponding to the MgCu$_2$-type (C15) Laves structure ($Fd3m$ space group). Magnetization measurements were performed on loose powders by using both commercial (Quantum Design) superconducting quantum interference device-MPMS5 and physical property measurement system magnetometers in magnetic fields up to 5 and 9 T, respectively. In all the cases, samples were zero-field cooled down to 4.2 K and the magnetization vs temperature curves were recorded on heating.

XMCD experiments were performed at the beamline BL39XU of the SPring8 Facility.[27] Undulator radiation, linearly polarized in the orbit plane, was monochromatized by a Si(111) fixed-exit double-crystal monochromator and higher harmonics rejected by a Pt-coated mirror. Circularly polarized x rays were generated using a 0.73-mm-thick diamond x-ray phase plate.[28] The degree of circular polarization is more than 90% in the energy range of our interest. XMCD spectra were recorded in the transmission mode at both Co K edge and Lu $L_{2,3}$ edges using the helicity-modulation technique.[29] Therefore, the sample is magnetized by an external magnetic field, applied in the direction of the incident beam, and the helicity is changed from positive to negative at each energy point. Consequently, XMCD spectra are obtained without reversing the applied magnetic field. The XMCD spectrum corresponds to the spin-dependent absorption coefficient obtained as the difference of the absorption coefficient $\mu_c=(\mu^- - \mu^+)$ for antiparallel, μ^-, and parallel,

μ^+, orientation of the photon helicity and the magnetic field applied to the sample. For the sake of accuracy the direction of the applied magnetic field is reversed and the XMCD, now $\mu_c=(\mu^+ - \mu^-)$, is recorded again by switching the helicity. The subtraction of the XMCD spectra recorded for both field orientations cancels, if present, any spurious signal.

For the measurements, homogeneous layers of the powdered samples were made by spreading fine powders of the material on an adhesive tape. The thickness and homogeneity of the samples were optimized to obtain the best signal-to-noise ratio. The XMCD spectra were recorded at $T=5$ K, the maximum applied magnetic field being $H=10$ T. The absorption spectra were analyzed according to standard procedures.[30,31] The origin of the energy scale, E_0, was defined as the inflection point of the absorption edge. The spectra were normalized to the averaged absorption coefficient at high energy, μ_0, in order to eliminate the dependence of the absorption on the sample thickness.

III. RESULTS AND DISCUSSION

A. Macroscopic magnetic measurements

The temperature dependence of the magnetization of the Y(Co$_{1-x}$Al$_x$)$_2$, Lu(Co$_{0.9}$Al$_{0.1}$)$_2$ and (Y$_{1-y}$Lu$_y$)(Co$_{0.88}$Al$_{0.12}$)$_2$ compounds is shown in Fig. 1. In the case of Y(Co$_{1-x}$Al$_x$)$_2$ magnetic ordering transitions are clearly observed for compounds with $x \geq 0.13$, while for compounds with Al concentrations below $x \leq 0.11$ no magnetic order is found. Magnetization vs applied magnetic field curves, $M(H)$, and Arrot plots, M^2 vs H/M, indicate that ferromagnetism is stabilized only for $x \geq 0.13$. In agreement with previous works, the Co magnetic moment, derived from the value of the magnetization at $H=5$ T, reaches its maximum value for $x=0.15$ and it progressively decreases upon further Al substitution (see Table I). In the case of Lu(Co$_{1-x}$Al$_x$)$_2$ the critical Al concentration for the onset of ferromagnetism has been previously reported to be within the range $0.06 \leq x \leq 0.1$.[6,20] However, recent studies have shown that the onset of ferromagnetism strongly depends on annealing due to the coexistence of paramagnetic and ferromagnetic states of Co atoms for $x \lesssim 0.08$.[19,32] Therefore, we have focused our study on the $x=0.1$ compound for which the maximum μ_{Co} within this series occurs.[18] In this case, the $M(H)$ curve shows a magnetic state approaching saturation, the magnetization per Co atom being $0.6\mu_B$ at $H=5$ T. Finally, (Y$_{1-y}$Lu$_y$)(Co$_{0.88}$Al$_{0.12}$)$_2$ compounds with $y=0.2$, 0.4, and 0.6 exhibit ferromagnetic behavior. While T_C increases linearly with the Lu content, a different behavior is found regarding the μ_{Co} values.[12,18] For low Lu content ($y=0.2$) the system exhibits all the hallmarks of a WFM. The magnetization per Co atom, μ_{Co}, increases linearly with the applied magnetic field, being $\sim 0.3\mu_B$ at 5 T. By contrast the richest Lu compound ($y=0.6$) shows a saturated magnetic state with $\mu_{Co} \sim 0.6\mu_B$. In the case of the intermediate content, $y=0.4$, the system evolves under the action of an applied magnetic field from WFM to SFM behavior.[2]

The complex magnetic behavior induced by the Al substitution in the three classes of compounds is usually discussed
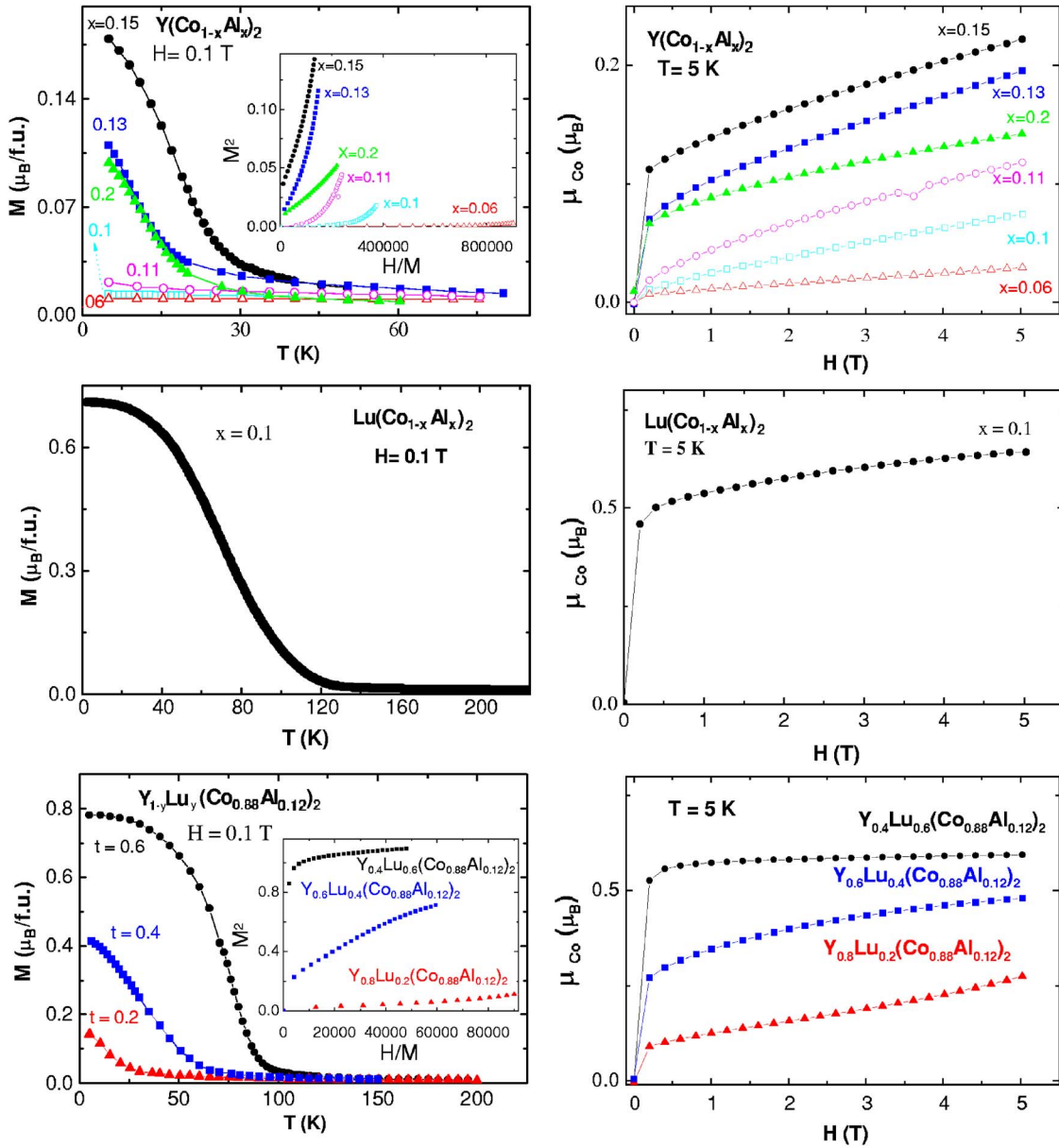
FIG. 1. (Color online) Left: Dependence of the magnetization vs temperature in the case of $Y(Co_{1-x}Al_x)_2$ (top panel), $Lu(Co_{1-x}Al_x)_2$ (middle), and $(Y_{1-y}Lu_y)(Co_{0.88}Al_{0.12})_2$ systems (bottom). In the case of the systems containing Y, Arrot plots (recorded at $T=5$ K) are shown in the insets. Right: Dependence of the magnetization, per Co atom, on the applied magnetic field.

in terms of the electronic modification of the systems. Inspection of the cell parameters of the $(Y_{1-y}Lu_y)(Co_{1-x}Al_x)_2$ compounds, summarized in Table I, indicates that the effect of Al substitution is not simply linked to the narrowing of the DOS. Indeed, while magnetic WFM and SFM ordering is stabilized as the cell parameter increases in $Y(Co_{1-x}Al_x)_2$ and $Lu(Co_{1-x}Al_x)_2$, respectively, the opposite occurs for the $(Y_{1-y}Lu_y)(Co_{0.88}Al_{0.12})_2$ series. Consequently, the complexity of this magnetic behavior cannot be simply attributed to the increase of the DOS at the Fermi level due to the narrowing of the density of states. On the contrary, it suggests that there is an interplay between this structural effect and the Al-induced modification of the DOS through the Co-Al hybridization.

This scenario poses the need for obtaining further knowledge of this interplay. X-ray absorption spectroscopy suits this purpose well as it is a simple and sensitive probe of the local unoccupied states, of a given symmetry, around the selected absorbing atomic species.[33] Consequently, we have extended our study to the analysis of the XAS and XMCD spectra at the Co K edge and Lu $L_{2,3}$ edges in the $(Y_yLu_{1-y})(Co_{1-x}Al_x)_2$ systems.

B. Co K edge XAS and XMCD

The near-edge region of the absorption spectrum is extremely sensitive to the modification of the DOS, while the high-energy region of the spectrum is related to the local

TABLE I. Structural and magnetic parameters of the $(Y_{1-y}Lu_y)(Co_{1-x}Al_x)_2$ compounds: lattice constant (a); magnetization measured at 5 T($M_{5\ T}$), and the Co moment derived from the magnetization data at $H=5$ T and $T=5$ K.

Compound	a (Å)	$M_{5\ T}$ (μ_B/f.u.)	μ_{Co} (μ_B/f.u.)
$Y(Co_{1-x}Al_x)_2$			
$x=0.06$	7.2541(4)	0.055	0.029
$x=0.10$	7.2759(4)	0.134	0.074
$x=0.11$	7.2849(3)	0.210	0.118
$x=0.13$	7.2982(3)	0.340	0.195
$x=0.15$	7.3014(3)	0.378	0.222
$x=0.20$	7.3247(5)	0.228	0.143
$Lu(Co_{1-x}Al_x)_2$			
$x=0.10$	7.1680(2)	1.156	0.642
$(Y_{1-y}Lu_y)(Co_{0.88}Al_{0.12})_2$			
$y=0.2$	7.2617(3)	0.485	0.276
$y=0.4$	7.2375(3)	0.845	0.480
$y=0.6$	7.2218(3)	1.047	0.595

structure around the absorbing atom. In order to discern the origin, structural vs electronic, of the differences in the absorption spectra it is instructive to compare the XAS spectra recorded at different applied fields on the same compound. In this way, Fig. 2 reports the comparison between the Co K edge spectra recorded at $H=5$ and 10 T in the case of $Y(Co_{0.85}Al_{0.15})_2$. As the crystal structure is retained, the difference between both absorption spectra shows the energy region that is mainly affected by the modification of the DOS. As shown in Fig. 2 these differences lie in the first 15 eV of the spectrum, i.e., at the raising edge region. For the sake of completeness, we have compared this difference to the XMCD spectra recorded at the same applied fields. As shown in the figure, the main features of the XMCD spectra lie at the same region as above where, in addition, the maximum modification of their intensity as a function of the applied magnetic field is found. Consequently, it is possible to address that differences in this energy region reflect the different magnetic states of the systems, as determined from a different DOS, while those in the high-energy region are related to structural effects.

Once we have determined the energy range of the absorption spectrum in which electronic effects are expected to dominate over structural ones, we have focused our study to monitor the proposed change of the Co magnetic ground state from weak (WFM) to strong (SFM) in the $(Y_yLu_{1-y})(Co_{1-x}Al_x)_2$ compounds as a function of the Y, Lu, and Al concentration. To this end, we have compared the normalized Co K edge XMCD spectra of $Y(Co_{0.85}Al_{0.15})_2$ and hcp cobalt. As shown in Fig. 2 the magnitude of the XMCD signals suggests that the magnetic ground state of Co is different in both systems. Indeed, while μ_{Co} in hcp cobalt is $\sim 1.7\mu_B$, it is only $\sim 0.2\mu_B$ in $Y(Co_{0.85}Al_{0.15})_2$. It should be noted that the spectrum in the Y compound has been recorded at 5 K and under the application of a 10 T magnetic field, while the reference was measured at room temperature
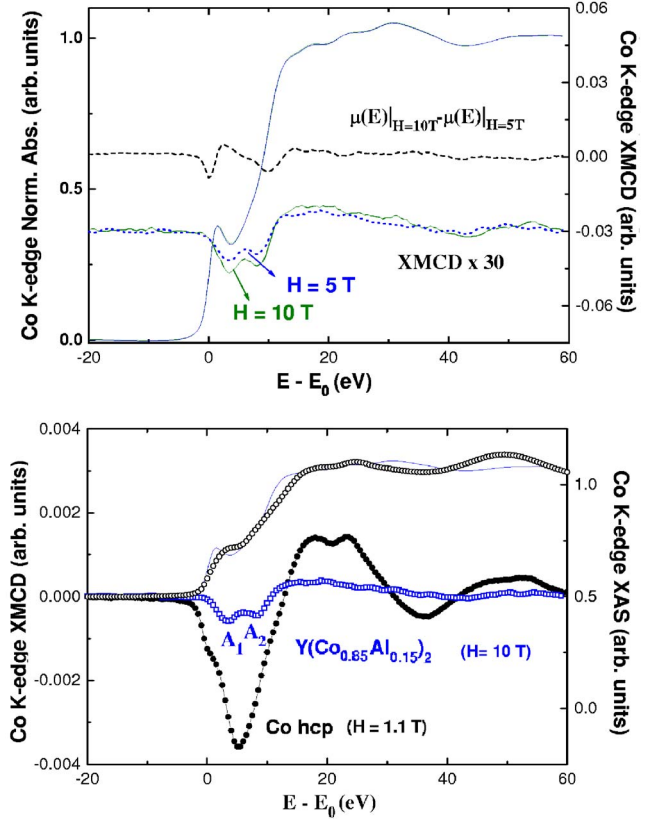

FIG. 2. (Color online) Top panel: Comparison of the Co K edge XMCD spectra of $Y(Co_{0.85}Al_{0.15})_2$ recorded at $H=5$ (blue dots) and 10 T (green solid line) and the difference of the XAS spectra recorded with the same applied magnetic fields (black dashed line). For sake of comparison the normalized Co K edge XAS spectrum recorded at $H=5$ (blue solid line) is also shown. Bottom panel: Comparison of the normalized Co K edge XMCD spectra of $Y(Co_{0.85}Al_{0.15})_2$ ($\square$, blue) and hcp cobalt ($\bullet$, black). For sake of clarity, the normalized Co K-edge XAS spectra are also shown: $Y(Co_{0.85}Al_{0.15})_2$ (solid line, blue); hcp cobalt (open circles, black).

and by applying a magnetic field of 1 T. The XMCD spectral shape is markedly different in both cases. Hcp Co shows a main broad negative peak extending over the first 17 eV with a shoulderlike feature at $E=0$ eV that coincides with the inflection point of the XAS spectrum. By contrast, the XMCD of the Y-based compounds exhibits two well-resolved negative peaks (A_1 and A_2) in the same energy region.

In a first approach, one can expect that the shape of the Co K edge XMCD spectrum evolves from that of $Y(Co_{0.85}Al_{0.15})_2$ to that of hcp cobalt, as the magnetic ground state of Co changes from weak (Y rich) to strong ferromagnetism character (Lu rich) throughout the $(Y_yLu_{1-y})(Co_{1-x}Al_x)_2$ series. Indeed, such a class of modification has been previously reported in the case of Fe-P amorphous alloys.[34] As the P concentration increases the system changes from WFM to SFM character and the shape of the Fe K edge XMCD evolves from that of bcc Fe to resemble that of hcp Co. However, this is not the case here. Figure 3 shows the dependence of the Co K edge XMCD as a function of the applied field in $Y(Co_{0.85}Al_{0.15})_2$, $(Y_{0.8}Lu_{0.2})(Co_{0.88}Al_{0.12})_2$, and $(Y_{0.4}Lu_{0.6})(Co_{0.88}Al_{0.12})_2$. As
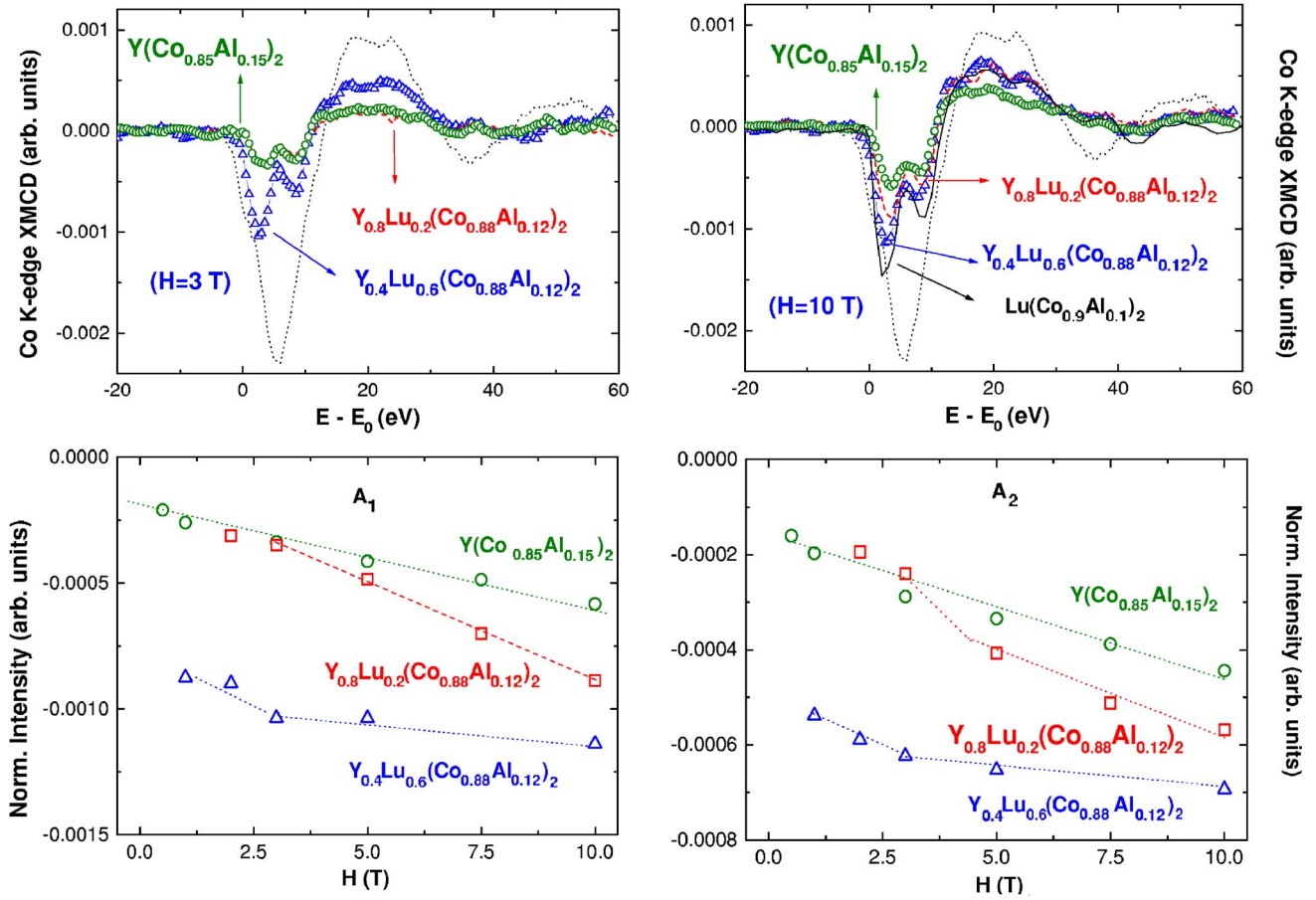
FIG. 3. (Color online) Upper panels: Comparison for different applied magnetic fields of the normalized Co K edge XMCD spectra of $Y(Co_{0.85}Al_{0.15})_2$ (green ○), $(Y_{0.8}Lu_{0.2})(Co_{0.88}Al_{0.12})_2$ (red dashed line) and $(Y_{0.4}Lu_{0.6})(Co_{0.88}Al_{0.12})_2$ (blue △). For the sake of clarity, the normalized Co K edge XMCD spectra of both hcp Co recorded at $H=1$ T (black dotted line) and $Lu(Co_{0.9}Al_{0.1})_2$ recorded at $H=10$ T (black solid line) are also shown. Lower panels: Dependence of the main XMCD features A_1 and A_2 on the magnetic applied field: $Y(Co_{0.85}Al_{0.15})_2$ (green ○), $(Y_{0.8}Lu_{0.2})(Co_{0.88}Al_{0.12})_2$ (red □), and $(Y_{0.4}Lu_{0.6})(Co_{0.88}Al_{0.12})_2$ (blue △). The dotted lines are guides for the eyes.

shown in the figure, the shape of the XMCD signals is the same for both Y-rich and Lu-rich compounds, i.e., for compounds showing WFM and SFM magnetic behavior, respectively. Moreover, in all the cases the XMCD spectrum is clearly different from that of hcp cobalt. Therefore, it is concluded that the particular shape of the XMCD spectra is mainly determined by the details of the DOS and not by the magnetic character of the Co atoms. Indeed, although all the signals show similar XMCD shape, their intensities clearly reflect the different magnetic (WFM vs SFM) regime. The Y-rich compounds show a small XMCD signal whose intensity grows linearly as the magnetic field is increased. This behavior reflects its weak itinerant ferromagnetic nature. By contrast, the XMCD of the richest Lu compound, $(Y_{0.4}Lu_{0.6})(Co_{0.88}Al_{0.12})_2$, (i) is significantly greater than for the Y-rich compounds, and (ii) its magnitude remains nearly constant when varying the applied magnetic field. This is shown in Fig. 3 where the dependence of the intensity of the characteristic XMCD spectral features, A_1 and A_2, is plotted as a function of the magnetic field. The behavior of $Y(Co_{0.85}Al_{0.15})_2$ can be assigned as corresponding to a weak itinerant ferromagnet while that of $(Y_{0.4}Lu_{0.6})(Co_{0.88}Al_{0.12})_2$ corresponds to a SFM material. By contrast, the behavior of

$(Y_{0.8}Lu_{0.2})(Co_{0.88}Al_{0.12})_2$ shows the hallmarks of a WFM-SFM transition. Indeed, at low applied fields its XMCD intensity matches that of the WFM $Y(Co_{0.85}Al_{0.15})_2$, while for $H>3$ T it departs from the WFM behavior, approaching the SFM one.

This is clearly observed when the normalized XMCD intensities are compared to the macroscopic magnetization data. As shown in Fig. 4, both XMCD and $M(H)$ data perfectly scale for applied fields $H≥3$ T. In the case of $(Y_{0.4}Lu_{0.6})(Co_{0.88}Al_{0.12})_2$ the values of the XMCD intensity obtained for low applied fields $H=1$ and 2 T are below the magnetization curve. We think this is related to the different signal-to-noise ratio that improves as the applied magnetic field, and consequently the XMCD intensity, increases. Indeed, the dependence of the XMCD intensity of both A_1 and A_2 features is different for these two points (see lower panels in Fig. 3). For the sake of completeness we have also included the data for the $Lu(Co_{0.9}Al_{0.1})_2$ compound although its XMCD has been recorded only at $H=10$ T. The values of μ_{Co} derived from the magnetization data at 9 T are $0.30\mu_B$, $0.47\mu_B$, and $0.61\mu_B$ for $Y(Co_{0.85}Al_{0.15})_2$, $(Y_{0.8}Lu_{0.2})(Co_{0.88}Al_{0.12})_2$, and $(Y_{0.4}Lu_{0.6})(Co_{0.88}Al_{0.12})_2$, respectively. For $Lu(Co_{0.9}Al_{0.1})_2$ the same procedure yields
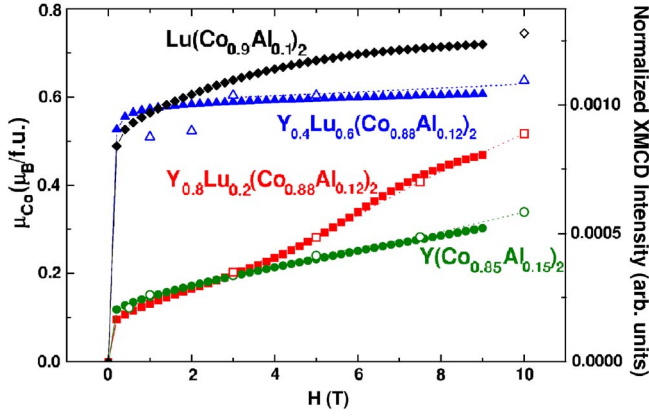
FIG. 4. (Color online) Comparison of the dependence on the magnetic applied field of the magnetization per cobalt atom (solid symbols) and the intensity of the A_1 feature in the Co K edge XMCD (open symbols) in the case of $Y(Co_{0.85}Al_{0.15})_2$ (green ○), $(Y_{0.8}Lu_{0.2})(Co_{0.88}Al_{0.12})_2$ (red □), $(Y_{0.4}Lu_{0.6})(Co_{0.88}Al_{0.12})_2$ (blue △, ▽), and $Lu(Co_{0.9}Al_{0.1})_2$ (black ◇). The dotted lines are guides for the eyes.

$\mu_{Co} = 0.7\mu_B$. Therefore, μ_{Co} appears to be "saturated" in the Y-Lu compound with the maximum Lu content, $(Y_{0.4}Lu_{0.6})(Co_{0.88}Al_{0.12})_2$, while that with the lowest Lu content, $(Y_{0.8}Lu_{0.2})(Co_{0.88}Al_{0.12})_2$, evolves from the Y-rich WFM toward the SFM state as the applied magnetic field increases.

C. Lu $L_{2,3}$ edge XMCD

The XMCD results evidence that there is no direct relationship between the different behavior of μ_{Co} and the cell parameters in both WFM and SFM compounds. The occurrence of the SFM state seems to be favored by increasing Lu concentration. This behavior has been tentatively attributed to the different hybridization between Co(3d) and Y(4d) and Co(3d) and Lu(5d).[19,21–23] Moreover, it has also been suggested that the Co(3d)-Al(p) hybridization modifies the shape of the characteristic peak of the YCo₂ DOS in such a way that upon increasing Al content $N(E_F)$ increases and weak ferromagnetism is favored.[13,14] However, even though the near-edge region is extremely sensitive to the modification of the DOS, no significant difference of either the XAS or XMCD signal is found at the Co K edge throughout the $(Y_yLu_{1-y})(Co_{1-x}Al_x)_2$ series.

Trying to get a deeper insight into the origin of this puzzle, we have explored the possibility of this magnetic behavior being due to the development of a magnetic moment at the Lu sites. With this aim we have extended our study to the case of the Lu $L_{2,3}$ absorption edges. It should be noted that, as previously shown,[35] the intensity of the Lu XMCD is greater at the L_2 than at the L_3 edge.[36] In addition, the experimental XMCD signals are weak due to the induced nature of the 5d magnetic moment. For these reasons we have mainly focused the discussion on the differences observed at the Lu L_2 edge.

In the case of the SFM compounds $Lu(Co_{0.9}Al_{0.1})_2$ and $(Y_{0.4}Lu_{0.6})(Co_{0.88}Al_{0.12})_2$ the XMCD intensity does not vary on increasing the applied magnetic field (see Fig. 5). On the

contrary, it shows a linear variation with the field in the case of the WFM $(Y_{0.8}Lu_{0.2})(Co_{0.88}Al_{0.12})_2$. These results point out that Lu bears a magnetic moment μ_{Lu} in all the studied compounds. Moreover, they show that the behavior of the Lu XMCD signals, and thus of μ_{Lu}, is different in the WFM and SFM systems. This is shown in Fig. 6 where the Lu L_2 XMCD signals for the investigated compounds are compared at low (3 T) and high (10 T) magnetic fields. The Lu magnetic moment appears to be saturated in both $Lu(Co_{0.9}Al_{0.1})_2$ and $(Y_{0.4}Lu_{0.6})(Co_{0.88}Al_{0.12})_2$ compounds, which are considered to be strong ferromagnetic materials. By contrast, small XMCD signals are obtained at low magnetic fields for $(Y_{0.8}Lu_{0.2})(Co_{0.88}Al_{0.12})_2$. However, as the applied magnetic field increases the XMCD intensity of $(Y_{0.4}Lu_{0.6})(Co_{0.88}Al_{0.12})_2$ approaches the values shown by the SFM materials. This result is in agreement with the existence of a WFM-to-SFM transition induced by the external field that is also inferred from the analysis of the Co K edge XMCD.

This can be clearly observed in Fig. 7 where the maximum of the L_2 XMCD intensity ($E=0$ eV) is plotted vs the applied magnetic field. The XMCD intensity remains nearly constant for the SFM compounds $(Y_{0.4}Lu_{0.6})(Co_{0.88}Al_{0.12})_2$ and $Lu(Co_{0.9}Al_{0.1})_2$, while it markedly increases ($\sim150\%$) with the field for the WFM compound. This behavior is in agreement with that obtained at the Co K edge, showing a relative $\sim10\%$ and 150% increase for the SFM and WFM compounds, respectively. It is interesting to note that in the case of compounds without Lu, such as $Y(Co_{0.85}Al_{0.15})_2$, the increase of the magnetization per Co atom is only 73%. This result suggests that, even though the Lu moment is induced by the Co one, its presence feeds the enhancement of the Co one by reinforcing the strong ferromagnetic character of the system.

Finally, aiming to get a relationship between μ_{Lu} and μ_{Co} we have performed a sum-rule analysis of the XMCD spectra. These sum rules have been derived by connecting the integrated XMCD spectra at the $L_{2,3}$ edges of Lu with the ground-state expectation value of both $\langle L_z \rangle$ and $\langle S_z \rangle$ of the 5d states:[24,25]

$$\langle L_z \rangle = 2 \times (A_{L_3} + A_{L_2}) \times \frac{n_h}{\mu}, \tag{1a}$$

$$\langle S_z \rangle + \frac{7}{2}\langle T_z \rangle = \frac{3}{2} \times (A_{L_3} - 2 \times A_{L_2}) \times \frac{n_h}{\mu}, \tag{1b}$$

where A_{L_3} and A_{L_2} are the integrals over the dichroic signal at the L_3 and L_2 edges, respectively. n_h is the number of holes in the Lu 5d band and μ is the unpolarized $L_{2,3}$ edge cross section after subtraction of a double step function that ideally models the contribution of the continuum states (see Fig. 8). No normalization to the absorption jump has been done either in the L_3 or the L_2 edge spectra in order to preserve the direct applicability of the sum rules. This analysis has been performed under the following assumptions: (i) μ is approximated by $\frac{3}{2}(\mu^+ + \mu^-)$; (ii) $\langle T_z \rangle$ is assumed to be negligible in the spin sum rule; (iii) estimates of both the orbital $\langle L_z \rangle$ and
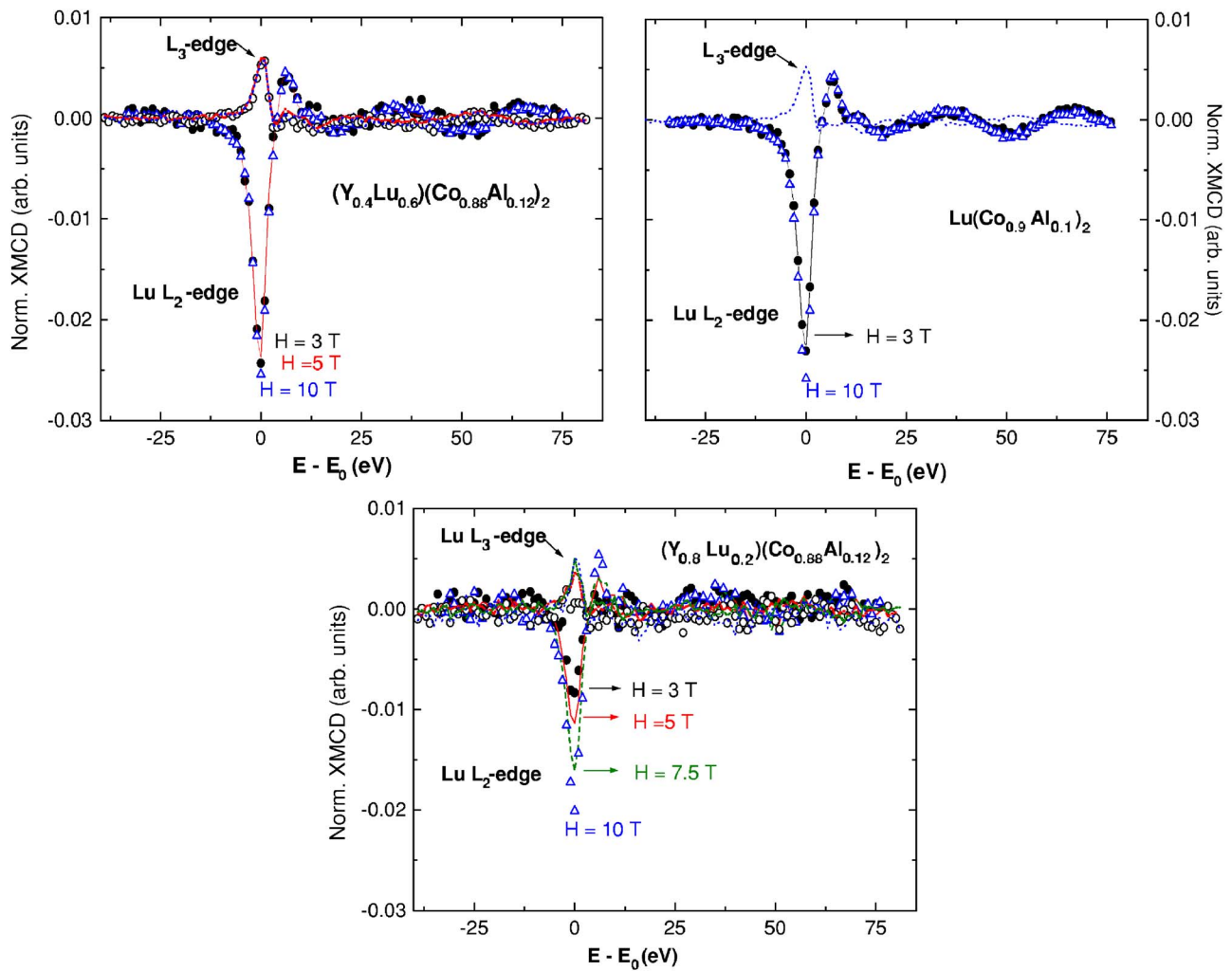
FIG. 5. (Color online) Dependence of the normalized Lu L_2 edge XMCD signals with the applied magnetic field in the case of Lu(Co$_{0.9}$Al$_{0.1}$)$_2$, (Y$_{0.4}$Lu$_{0.6}$)(Co$_{0.88}$Al$_{0.12}$)$_2$, and (Y$_{0.8}$Lu$_{0.2}$)(Co$_{0.88}$Al$_{0.12}$)$_2$. XMCD spectra were recorded at $T=5$ K and with a fixed applied field of 3 T (black •), 5 (red solid line), 7.5 (green dashed line), and 10 T (blue △). For the sake of completeness the L_3 edge XMCD spectra are also shown: $H=3$ (black ∘), 5 (red dot-dashed line), 7.5 (green short-dashed line), and 10 T (blue dotted line).
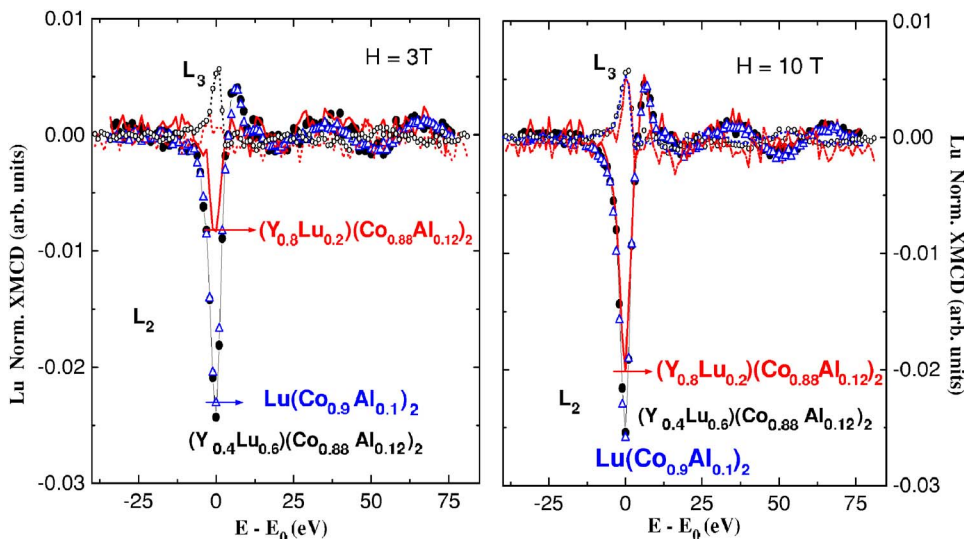

FIG. 6. (Color online) Comparison of the normalized Lu L_2 edge XMCD signals recorded at $H=3$ (left panel) and 10 T (right panel): Lu(Co$_{0.9}$Al$_{0.1}$)$_2$ (blue △), (Y$_{0.4}$Lu$_{0.6}$)(Co$_{0.88}$Al$_{0.12}$)$_2$ (black •), and (Y$_{0.8}$Lu$_{0.2}$)(Co$_{0.88}$Al$_{0.12}$)$_2$ (red solid line). For the sake of completion the L_3 edge XMCD spectra are also shown: Lu(Co$_{0.9}$Al$_{0.1}$)$_2$ (blue dashed line), (Y$_{0.4}$Lu$_{0.6}$)(Co$_{0.88}$Al$_{0.12}$)$_2$ (black ∘), and (Y$_{0.8}$Lu$_{0.2}$)(Co$_{0.88}$Al$_{0.12}$)$_2$ (red dotted line).
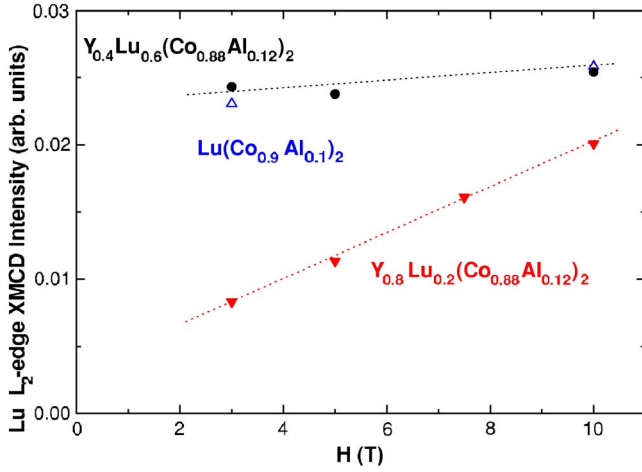
FIG. 7. (Color online) Modification of the maximum of the Lu L_2 edge XMCD signals as a function of the applied magnetic field: Lu$(Co_{0.9}Al_{0.1})_2$ (blue $\triangle$), $(Y_{0.4}Lu_{0.6})(Co_{0.88}Al_{0.12})_2$ (black •), and $(Y_{0.8}Lu_{0.2})(Co_{0.88}Al_{0.12})_2$ (red ▼).

spin $\langle S_z \rangle$ moments have been derived by considering $n_h = 9$. These approximations can be rather crude in order to get a correct estimate of the magnetic moment. Even though the absolute value of the $5d$ Lu magnetic moment derived from the XMCD spectra has to be considered with some caution, the trend of its modification, obtained by using the same parameters, through the whole series of compounds studied is not seriously affected.

The values of both the orbital and spin moments of the Lu $5d$ states are summarized in Table II. For the sake of comparison the data of LuFe$_2$ are also shown. In all the cases the induced moment at the Lu sites is of opposite sign to that of Co, in agreement with band-structure calculations.[11,37,38] In the case of LuFe$_2$, theoretical calculations by Yamada and Shimizu have predicted a $5d$ μ_{Lu} moment of $-0.33\mu_B$,[37] while calculations by Brooks *et al.* yield a $-0.41\mu_B$ moment at the Lu sites of which $-0.27\mu_B$ is of partial $5d$ character.[38] The existence of an ordered moment at the lutetium sites was early confirmed[39] by XMCD although no estimates of its value were reported. For this compound, our data yield $\mu_{Lu} \sim 0.13\mu_B$, a value significantly smaller than that theoretically predicted. The different magnitude of the Lu moment estimates derived from the XMCD and band calculations is probably due to the strong approximations included in the sum-rule analysis and to the fact that band calculations are reserved for ideal systems. Notwithstanding the different magnitude, both band calculations and XMCD data yield the same coupling scheme for the $3d$ magnetic moment of Co and the Lu $5d$ one. Indeed, similar ferrimagnetic coupling is found between the Co and Lu moments in the studied Lu$(Co_{0.9}Al_{0.1})_2$ and $(Y_{1-y}Lu_y)(Co_{0.88}Al_{0.12})_2$ compounds. However, the maximum μ_{Lu} found, $\sim 0.05\mu_B$, is half that of the LuFe$_2$ case. This result agrees with the fact that the Lu magnetic moment is induced by that of the transition metal in both Fe and Co compounds, since $\mu_{Co} < \mu_{Fe}$. Moreover, the XMCD data show that this induced μ_{Lu} is near saturated, in the range $\sim (0.05-0.06)\mu_B$, in those compounds, showing strong ferromagnetic behavior as in Lu$(Co_{0.9}Al_{0.1})_2$ and
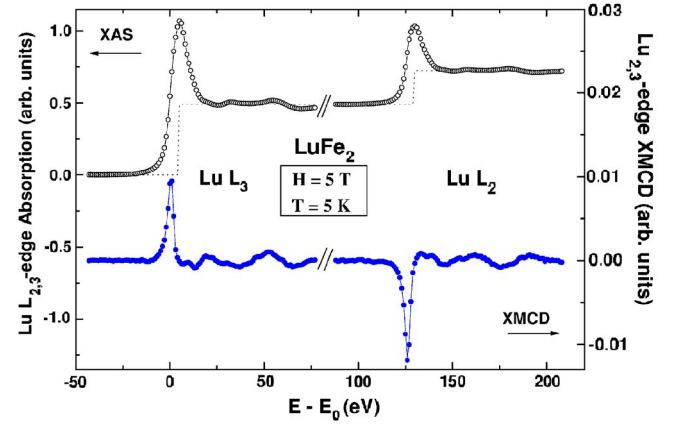

FIG. 8. (Color online) Lu $L_{2,3}$ edge XMCD (blue •) and XAS (black ∘) spectra of LuFe$_2$ as used for the sum-rule application. No normalization has been applied and the L_2 XAS spectrum has been vertically shifted to match the L_3 one. The dotted line shows the two-step-like function used to obtain the d-state isolated spectra.

$(Y_{0.4}Lu_{0.6})(Co_{0.88}Al_{0.12})_2$. By contrast, the WFM systems $(Y_{0.8}Lu_{0.2})(Co_{0.88}Al_{0.12})_2$ and Lu$(Co_{0.93}Al_{0.07})_2$ show a reduced $(\sim 0.01\mu_B)\mu_{Lu}$ at low applied magnetic field which increases, approaching $(\sim 0.04\mu_B)$ the "saturated" value at $H = 10$ T.

A final comment is deserved on the relationship between the existence of a magnetic moment at the Lu sites and the *Lu paradox*.[23,40] This refers to the unusual magnetic behavior

TABLE II. Estimates (in μ_B) of the ground-state expectation value of the orbital, $\langle L_z \rangle$, and spin, $\langle S_z \rangle$, moment of the Lu $5d$ states derived from the XMCD sum-rule analysis at $T = 5$ K. The uncertainty of these values is estimated to be 15%.

Compound	3 T	5 T	7.5 T	10 T
$(Y_{0.8}Lu_{0.2})(Co_{0.88}Al_{0.12})_2$				
$\langle L_z \rangle$	-0.004	-0.003	-0.007	-0.010
$\langle S_z \rangle$	0.008	0.015	0.022	0.025
$\mu_{Lu} \rangle | 5d$	-0.012	-0.027	-0.037	-0.040
$(Y_{0.4}Lu_{0.6})(Co_{0.88}Al_{0.12})_2$				
$\langle L_z \rangle$	-0.009	-0.010		-0.010
$\langle S_z \rangle$	0.031	0.032		0.034
$\mu_{Lu} \rangle | 5d$	-0.053	-0.054		-0.058
Lu$(Co_{0.9}Al_{0.1})_2$				
$\langle L_z \rangle$				-0.003
$\langle S_z \rangle$				0.028
$\mu_{Lu} \rangle | 5d$				-0.053
LuFe$_2$ (300 K)				
$\langle L_z \rangle$		-0.002		
$\langle S_z \rangle$		0.049		
$\mu_{Lu} \rangle | 5d$		-0.096		
LuFe$_2$ (5 K)				
$\langle L_z \rangle$		-0.004		
$\langle S_z \rangle$		0.065		
$\mu_{Lu} \rangle | 5d$		-0.126		

of the $Lu(Co_{1-x}Al_x)_2$ systems showing magnetic ordering temperatures, ~ 150 K,[18] higher than that of the isostructural $R(Co_{1-x}Al_x)_2$ compounds for $x > 0.12$, where R is a magnetic heavy rare earth. By contrast, T_C does not exceed 30 K for $Y(Co_{1-x}Al_x)_2$.[4] These results have been tentatively attributed to differences of the d states in both Y and Lu compounds.[41] However, no theoretical computation confirms this fact and, consequently, its detailed explanation is lacking to date. The XMCD results indicate that the highest T_C occurs for those compounds showing an enhanced Lu moment, while μ_{Lu} is strongly reduced in those compounds showing low T_C. As discussed above, no clear relation exists among volume effects, differences of the d states in both Y and Lu compounds, and the high magnetic ordering temperature exhibited by the Lu-rich compounds. The results presented here point out that the developing of an ordered moment at the Lu sites is critical in favoring ferromagnetism through the reinforcement of the magnetic interactions in the system. Further work is needed to determine the role, if present, of an induced moment at the Y sites.

IV. SUMMARY AND CONCLUSIONS

The peculiar magnetic behavior of the $(Y_yLu_{1-y})(Co_{1-x}Al_x)_2$ systems has been studied by means of x-ray absorption spectroscopy and x-ray magnetic circular dichroism techniques.

The $Co\,K$ edge XMCD spectra of all the $(Y_yLu_{1-y})(Co_{1-x}Al_x)_2$ compounds studied is similar, independently of the magnetic character of the systems (WFM vs SFM), and markedly different from that of hcp Co. Even though the XMCD spectral shape is retained, its intensity reflects the different magnetic character of the systems and monitors the WFM-SFM transition. In particular, the Co magnetic moment seems saturated in $(Y_{0.4}Lu_{0.6})(Co_{0.88}Al_{0.12})_2$ while in the case of the low-Lu-content $(Y_{0.8}Lu_{0.2})(Co_{0.88}Al_{0.12})_2$ compound it evolves from the Y-rich WFM toward the SFM state as the applied magnetic field increases.

The XMCD at the Lu $L_{2,3}$ edges indicates the existence of an ordered $5d$ moment at the lutetium sites, ferrimagnetically coupled to the Co moment. Estimates of the Lu magnetic moment have been obtained by applying the XMCD sum rules. As in the case of the Co edge, the behavior of the Lu XMCD signals is clearly different in the WFM and SFM systems. For SFM compounds $\mu_{Lu} \sim 0.06\mu_B$ seems to be saturated. By contrast, μ_{Lu} increases from $\sim 0.01\mu_B$ to $\sim 0.04\mu_B$ as the applied magnetic field is increased. Present results indicate that the highest T_C occurs for those compounds showing an enhanced Lu moment, while μ_{Lu} is strongly reduced in those compounds showing low T_C. These results suggest that the existence of a Lu moment is critical in favoring ferromagnetism through the reinforcement of the magnetic interactions in the system.

To date, the peculiar magnetic behavior of the $(Y_yLu_{1-y})(Co_{1-x}Al_x)_2$ systems has been attributed to the modification of the DOS induced by Al, by qualitatively considering volume effects, a rigid band mechanism, or the change of the DOS shape due to the hybridization between the $Co(3d)$ and $Al(3p)$ states. By contrast, little attention has been given to the role played by both Y and Lu in contributing to the magnetic behavior. The present results show the different electronic impact of Al in the Y and Lu compounds; the induction of a $5d$ magnetic moment at the Lu sites and the way in which it varies through the WFM-SFM transition and as a function of different external parameters. This suggests the need of explicitly including both the $Co(3d)$-$Y(4d)$ and $Co(3d)$-$Lu(5d)$ hybridization in the theoretical description of the magnetic properties of these compounds. We think that these results can stimulate further theoretical work in order to get a proper understanding of these itinerant magnetic systems.

[1] T. Goto, H. A. Katori, T. Sakakibara, H. Mitamura, K. Fukamichi, and K. Murata, J. Appl. Phys. **76**, 6682 (1994).

[2] E. Gratz and A. Markosyan, J. Phys.: Condens. Matter **13**, R385 (2001).

[3] T. Goto, K. Fukamichi, T. Sakakibara, and H. Komatsu, Solid State Commun. **72**, 945 (1989).

[4] K. Yoshimura and Y. Nakamura, Solid State Commun. **56**, 767 (1985).

[5] T. Sakakibara, T. Goto, K. Yoshimura, M. Shiga, and Y. Nakamura, Phys. Lett. A **117**, 243 (1986).

[6] T. Sakakibara, T. Goto, K. Yoshimura, M. Shiga, Y. Nakamura, and K. Fukamichi, J. Magn. Magn. Mater. **70**, 126 (1987).

[7] H. Wada, K. Yoshimura, G. Kido, M. Shiga, M. Mekata, and Y. Nakamura, Solid State Commun. **65**, 23 (1988).

[8] T. Sakakibara, T. Goto, K. Yoshimura, and K. Fukamichi, J. Phys.: Condens. Matter **2**, 3381 (1990).

[9] V. V. Aleksandryan, A. S. Lagutin, R. Z. Levitin, A. S. Markosyan, and V. V. Snegirev, Sov. Phys. JETP **62**, 153 (1985).

[10] M. Cyrot and M. Lavagna, J. Phys. (France) **40**, 763 (1979).

[11] H. Yamada, J. Inoue, K. Terao, S. Kanda, and M. Shimizu, J. Phys. F: Met. Phys. **14**, 1943 (1984).

[12] I. L. Gabelko, R. Z. Levitin, A. S. Markosyan, V. I. Silant'ev, and V. V. Snegirev, J. Magn. Magn. Mater. **94**, 287 (1991).

[13] M. Aoki and Y. Yamada, Physica B **177**, 259 (1992).

[14] M. Aoki and Y. Yamada, J. Magn. Magn. Mater. **78**, 377 (1989).

[15] J. Y. Son, T. Konishi, T. Mizokawa, A. Fujimori, K. Koui, and T. Goto, Physica B **237-238**, 400 (1997).

[16] T. Sakakibara, H. Mitamura, and T. Goto, Physica B **201**, 127 (1994).

[17] S. Khmelevskyi, I. Turek, and P. Mohn, J. Phys.: Condens. Matter

13, 8405 (2001).

[18] I. L. Gabelko, R. Z. Levitin, A. S. Markosyan, and V. V. Snegirev, JETP Lett. **45**, 458 (1987).

[19] T. Yokoyama, H. Saito, K. Fukamichi, K. Manishima, T. Goto, and H. Yamada, J. Phys.: Condens. Matter **13**, 9281 (2001).

[20] M. Iijima, K. Endo, T. Sakakibara, and T. Goto, J. Phys.: Condens. Matter **2**, 10069 (1990).

[21] K. Fukamichi, T. Yokoyama, H. Saito, T. Goto, and H. Yamada, Phys. Rev. B **64**, 134401 (2001).

[22] I. S. Dubenko, R. Z. Levitin, A. S. Markosyan, V. V. Snegirev, and A. Y. Sokolov, J. Magn. Magn. Mater. **135**, 326 (1994).

[23] I. S. Dubenko, R. Z. Levitin, and A. S. Markosyan, J. Magn. Magn. Mater. **111**, 146 (1992).

[24] B. T. Thole, P. Carra, F. Sette, and G. van der Laan, Phys. Rev. Lett. **68**, 1943 (1992).

[25] P. Carra, B. T. Thole, M. Altarelli, and X. Wang, Phys. Rev. Lett. **70**, 694 (1993).

[26] J. Rodriguez-Carvajal, Physica B **192**, 55 (1993).

[27] H. Maruyama, J. Synchrotron Radiat. **8**, 125 (2001).

[28] K. Hirano, K. Izumi, T. Ishikawa, S. Annaka, and S. Kikuta, Jpn. J. Appl. Phys., Part 2 **30**, L407 (1991).

[29] M. Suzuki, N. Kawamura, M. Mizumaki, A. Urata, H. Maruyama, S. Goto, and T. Ishikawa, Jpn. J. Appl. Phys., Part 2 **37**, L1488 (1998).

[30] D. E. Sayers and B. A. Bunker, in *X-Ray Absorption: Principles,* *Applications, Techniques of EXAFS, SEXAFS, and XANES*, edited by D. C. Koningsberger and R. Prins (Wiley, New York, 1988), Chap. 6, and references therein.

[31] *X-Ray Absorption Fine Structure for Catalysts and Surfaces*, edited by Y. Iwasawa (World Scientific, Singapore, 1996).

[32] T. Yokoyama, H. Nakajima, H. Saito, K. Fukamichi, H. Mitamura, and T. Goto, J. Alloys Compd. **266**, 13 (1998).

[33] J. E. Müller and J. W. Wilkins, Phys. Rev. B **29**, 4331 (1984).

[34] M. L. Fdez-Gubieda, A. García-Arribas, J. M. Barandiarán, R. López Antón, I. Orue, P. Gorria, S. Pizzini, and A. Fontaine, Phys. Rev. B **62**, 5746 (2000).

[35] C. Giorgetti *et al.*, Phys. Rev. B **48**, 12732 (1993).

[36] C. Brouder and M. Hikam, Phys. Rev. B **43**, 3809 (1991).

[37] H. Yamada and M. Shimizu, J. Phys. F: Met. Phys. **16**, 1039 (1986).

[38] M. S. S. Brooks, O. Eriksson, and B. Johansson, J. Phys.: Condens. Matter **1**, 5861 (1989).

[39] F. Baudelet, C. Brouder, E. Dartyge, A. Fontaine, J. P. Kappler, and G. Krill, Europhys. Lett. **13**, 751 (1990).

[40] I. S. Dubenko, R. Z. Levitin, A. S. Markosyan, V. V. Snegirev, A. Y. Sokolov, and H. Yamada, J. Magn. Magn. Mater. **140-144**, 827 (1995).

[41] I. S. Dubenko, R. Z. Levitin, A. S. Markosyan, and H. Yamada, J. Magn. Magn. Mater. **136**, 93 (1994).